Oceanic Fronts and Related Phenomena (Konstantin Fedorov Memorial Symposium), Pushkin, 1998

SHORT FRONTAL WAVES: CAN FRONTAL INSTABILITIES GENERATE SMALL SCALE SPIRAL EDDIES?

T. Eldevik[1] and K. B. Dysthe[2]

Department of Mathematics, University of Bergen, J. Bruns gt. 12, 5008 Bergen, Norway
[1] Tor.Eldevik@mi.uib.no
[2] Kristian.Dysthe@mi.uib.no

Abstract. Small cyclonic spiral eddies with a scale of 10 km, are very frequently observed at the ocean surface, both from satellites and space shuttles. We are investigating whether their generation may be due to frontal instabilities, *i.e.* short scale cyclogenesis. The comparison of our numerical experiment to observations and linear stability analysis of two-layer frontal models, are promising. Spiraling short wave instabilities are clearly seen. The spiral eddies observed at the Almeria-Oran density front, among others, may possibly be explained by this model.

1. Introduction

At low wind speeds, a rich variety of surface structures are observed by remote sensing, particularly the so-called spiral eddies, with small scale, $O(10\,\text{km})$, spiraling structure. Up to the eighties, they were considered to be rare dynamic features in the ocean. Photographs of the world's oceans from space shuttles [1], and images of Norwegian coastal waters from radar satellites [2], have shown that such eddies are indeed common. In the former survey they are found to be always cyclonic, with a diameter of 12 to 15 km, while in the latter, 85% of the eddies were cyclones and 15% anti-cyclones. The average diameter of the anti-cyclonic eddies was more than three times that of the cyclones, which was estimated to be approximately 7 km. We therefore define spiral eddies to be of order 10 km, and from the observational material they are assumed to be cyclones. They are observed in many oceans in both hemispheres, but not in the vicinity of the Equator. This has lead us to the conclusion that the phenomenon is influenced by the rotation of the earth. It seems from the two surveys mentioned above that the dimensions of the cyclones decrease with increasing latitude. Although speculative, this is consistent with the Coriolis effect. The measures of length scales from the observations are approximate. The variation in diameter of the eddies may just as well be caused by different density stratifications at the different locations. It is also possible that their size changes during their evolution. Although not discussed herein, there are indications of the latter in our simulations [3].

The horizontal dimension of the spiral eddies is in the very low range of the internal radius of deformation in the ocean. If the background rotation is to play a part, stratification must be present and the dynamics restricted to an upper shallow layer of the ocean. Both moderate and large Rossby numbers, *Ro*, are estimated from the observations [4]. It has been proposed that the spiral eddies are the consequence of large (greater than unity) *Ro* dynamics [5]. As far as we understand, this work does not account for the generation of the eddies, but explains why there would be a preference for cyclonic eddies from an initial field of vortices of both orientations. In this regime, anti-cyclones are unstable from a mechanism akin to the so-called "centrifugal instability" [6]. The structures displayed in our simulations are of moderate Rossby number.

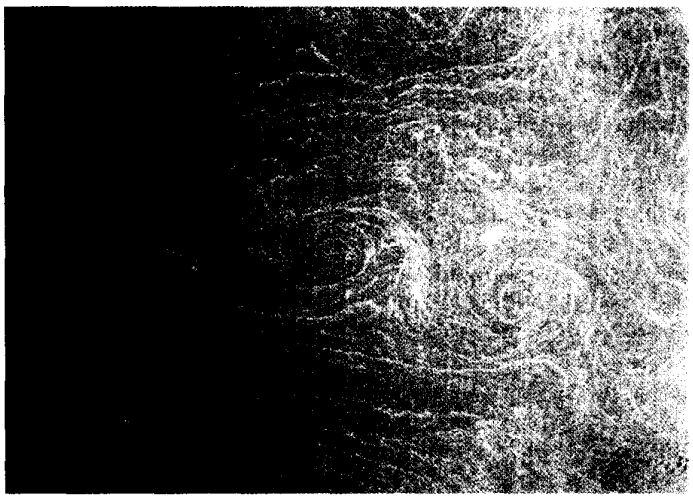

Figure 1: Photograph of spiral eddy street in the Mediterranean Sea off the coast of the Egyptian/Libyan border, from [4].

A beautiful eddy street is shown in Figure 1. The pattern is made visible by the sun's reflection from the surface of the sea, the sun glitter. The specular point is close to the center of the image. The relatively bright lines are thought to represent areas where the local roughness of the sea surface is smoother than the surrounding water [1]. The presence of surfactants are known to cause such slicks. It should be noted that the observed eddy patterns in general are more random than the one shown here.

Apart from understanding the phenomena as such, there are several other important reasons to study such submesoscale dynamics. They are often essential to the understanding of the larger system, but the dynamics of this scale are missing due to the coarse resolution of most numerical ocean models. The parameterization of sub-grid scale physical effects in numerical models is essential for their performance. The observations are, however, all snapshots. To our knowledge, there is no temporal data available for these features. Knowledge of how spiral eddies are generated, may improve the interpretation of satellite data. It has also been suggested [7], that cyclonic eddies are important in the development of frontal phytoplankton blooms.

2. Frontal instability as a generation mechanism

In geostrophic balance, the shear over a front separating water masses of different densities and velocities is cyclonic because of the thermal wind relation. Thus, there is a reservoir of cyclonic relative vorticity associated with the front that is essential for the deformation of the front when exposed to an unstable perturbation. This is one of the basic insights that led to the formulation of the celebrated cyclone model of the Bergen School [8] in meteorology. Also associated with frontal areas, is the presence of relatively strong horizontal convergence. At the ocean surface, this can lead to the accumulation of slicks.

The generation of spiral eddies through cyclogenesis at ocean fronts, could be the common denominator of the observations of [1] and [2]. The former author argue that the streaks trace out velocity shear and the latter authors claim that the eddies seem to be "situated exactly at the border between, in all probability, two different masses" in several of the images. A special case is found in the the Alboran Sea, between Spain and Algeria. At the same location where spiral eddies were observed from the space shuttle, *in situ* measurements later confirmed there to be an intense density front, the Almeria-Oran front [9]. This has led us to our working hypothesis that spiral eddies are surface signatures of small scale ocean frontal instabilities in regions of strong horizontal convergence.

A stationary geostrophic surface front in a two-layered fluid has been found to be linearly unstable to

short wavelength perturbations in the direction of the front when the pycnocline separating the two fluids of constant densities initially is assumed to be of constant slope [10, 11], parabolic [12], or exponential [13]. In these models, the fluid motion in each layer is governed by the non-viscous shallow water equations in an f-plane, and no external forcing is present. Under the amplification of a disturbance, energy is extracted from the available potential energy of the density distribution and the kinetic energy of the mean flow.

The initial assumption of a *parabolic* or an *exponential* profile can be related to simple physical arguments concerning the conservation of potential vorticity (PV). The former will be the result when the lighter fluid has been compressed to the surface from a large (infinite) thickness. Geostrophic adjustment of an originally motionless upper layer of uniform depth will produce the latter. In both these cases, the PV of the upper layer is uniform and there is relative vorticity present within the layer.

There does not seem to be any such basic argument available for choosing the initial pycnocline to have a *constant slope*, where the flow in each layer is uniform, but not the PV. Still, this will be the case of the numerical experiments described and discussed in the following. We have chosen to focus on the shear *across* the front. The streaks tracing out the spiral eddies are thought to be associated with a cyclonic shear of $O(10^{-3}\mathrm{s}^{-1})$ [1]. This is an order of magnitude larger than any relative vorticity that may be present *within* the layers, regardless of the initial profile. We suggest that this model is a near front approximation to the two conditions mentioned aboved.

3. The numerical experiment

The numerical experiment was performed with a three dimensional, primitive equation, σ-coordinate ocean model [14], the computational domain being a periodic channel in the x-direction, with a free surface and a flat bottom. In order to simulate the upper ocean layer, the boundary at the bottom was set to be stress-free. The initial geostrophic state (Figure 2) consists of two fluids of different uniform densities, separated by a pycnocline of constant slope (in the y-direction), intersecting both the bottom and the surface. The surface elevation and the steepness of the pycnocline is such that the upper (lighter) layer is flowing with a constant velocity in the positive x-direction and the lower layer is at rest. The

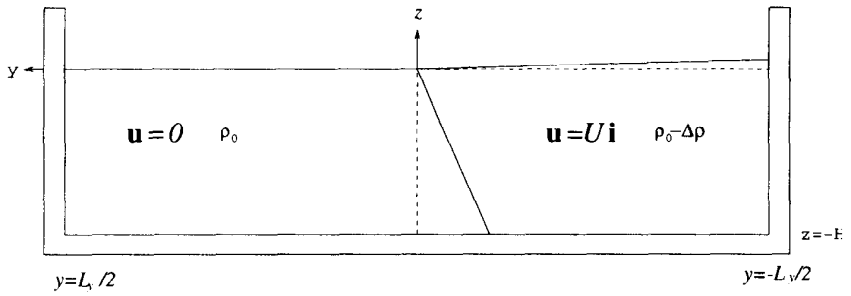

Figure 2: The initial geostrophic frontal configuration, the x-axis pointing inwards.

characteristics of the unperturbed geostrophic flow (at $t = 0$, see below) are given in Table , where R is the internal radius of deformation, U is the equilibrium geostrophic velocity of the upper layer, ρ_0 is the density of the heavier fluid, $\Delta\rho$ is the density difference between the two layers, f is the Coriolis parameter and H is the depth of the channel. The chosen values are not intended to represent any specific location,

R	U	ρ_0	$\Delta\rho$	f	H	L_x	L_y	Δx	N_σ	Δt
[km]	[m/s]	[kg/m^3]	[kg/m^3]	[1/s]	[m]	[km]	[km]	[km]		[s]
6.92	0.4	1025.0	1.0	10^{-4}	50.0	32.0	128.0	0.50	11	75.0

Table 1: The physical and numerical parameters governing the flow at $t = 0$.

but should be representative for a mid-latitude density front. L_x and L_y are the length and width of the channel, respectively. Decreasing the width by 25% yields no significant difference in the simulations for the times displayed herein, thus it is reasonable to state that the validity of the experiment is not restricted to coastal currents. The horizontal spatial step Δx, the number of σ-layers N_σ, and the time step Δt, give the resolution of the numerical scheme.

A strictly two-layered model is not possible to sustain in a three dimensional numerical model (nor in nature). The discontinuity that represents the front in the former model, will become continuous in the latter. The flows were therefore allowed to adjust to a state where further smoothing of the density and velocity profiles over the front was negligible, at which time ($t = 0$, say) they were perturbed. The effective horizontal diffusivities at the front in the simulations were estimated to be between 10 and $20\,\mathrm{m}^2/\mathrm{s}$. Such values affect only length scales much smaller than the scale of the spiral eddies. This keeps the front quite narrow and lets the instability set in, unaffected by dissipation. Thus the strong shear associated with the eddies are present, and a comparison with two-layer linear stability theory [11] is relevant.

It has been shown [10, 11] that for a given (two-layer) Richardson number,

$$Ri \equiv \frac{\Delta\rho}{\rho_0}\frac{gH}{U^2},$$

the linear stability of the geostrophic two-layer flow is determined by the perturbation Rossby number

$$Ro_k \equiv \frac{kU}{2f},$$

the prescribed (infinitesimal) perturbation with wavenumber k being in the direction of the flow. For the values of Table , $Ri = 3.0$. The most unstable perturbation is then predicted to be $Ro_k = 0.4$, amplifying with an e-folding time $T_e = 20\,\mathrm{h}$, through a mixed baroclinic/barotropic instability, dominated by the former [11]. This Rossby number corresponds to a wavelength equal to the chosen length of the channel, L_x.

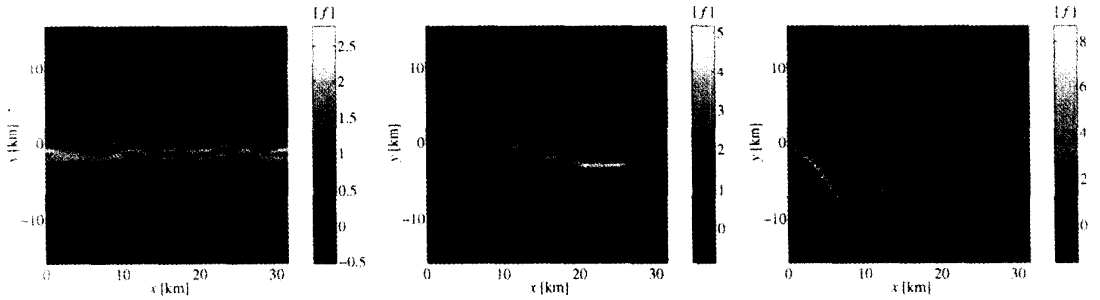

(a) $t = 84\,\mathrm{h}$. (b) $t = 120\,\mathrm{h}$. (c) $t = 156\,\mathrm{h}$.

Figure 3: The onset of instability and the generation of a spiral eddy as seen in the surface relative vorticity. The gray scale is related to the planetary vorticity f, and $y = 0$ is the initial position of the surface front.

The onset of instability in the experiment, initially perturbed with wavelengths L_x, $L_x/2$, and $L_x/4$ at $t = 0$, is shown for the surface relative vorticity in Figure 3. It is clearly seen that the dominant mode corresponds to the wavelength predicted above: in the early stages, Fig. 3(a), all wavelengths are clearly present, at the intermediate stage, Fig. 3(b), the wavelength L_x dominates and will soon be breaking. A control run with a channel of double length was made, and the most unstable perturbation was confirmed to be $Ro_k = 0.4$. In the last snapshot, Fig. 3(c), where nonlinear effects are clearly present, the front curls into a cyclonic spiral with a central patch of vorticity several times f.

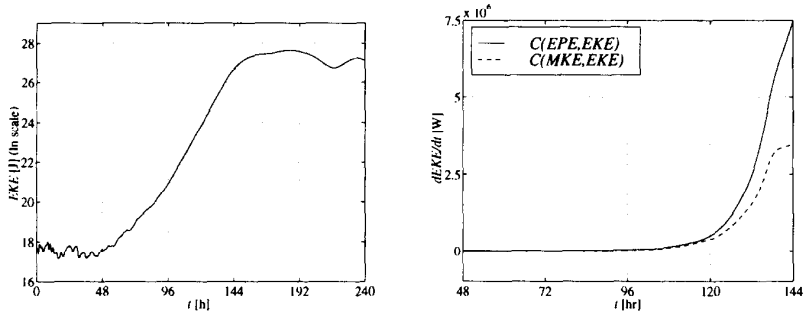

(a) The eddy kinetic energy.

(b) Energy conversion terms.

Figure 4: Energetics of the instability: (a) the EKE (ln scale) and (b) the conversion rate of energy into EKE from EPE, $C(EPE, EKE)$, and from MKE, $C(MKE, EKE)$, (linear scale).

The energetics of the instability, given by the eddy kinetic energy (EKE) and the rates of conversion of mean kinetic energy (MKE) and eddy potential energy (EPE) into EKE [15], are shown in Figure 4. From about $t = 48$ h to 144 h, the EKE shows an exponential growth (Fig. 4(a)), with an e-folding time of about 10 hours (corresponding to $T_e \approx 20$ h for the amplifying wave). In the same period, we see that EKE is extracted mainly from EPE, but there is also a contribution from MKE, Fig. 4(b). The former conversion constitutes a baroclinic instability, and the latter a barotropic instability. Thus the wavelength, growth rate, and energetics of the fastest growing wave are in good agreement with the linear theory [11].

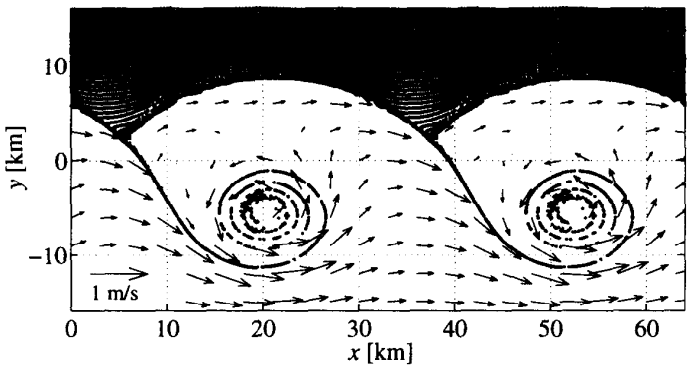

Figure 5: The spiral eddies displayed in the passive surface floats and the surface velocity field at $t = 168$ h. The periodic domain is shown twice.

In Figure 3, the onset of the instability and the birth of the spiral eddies are displayed in terms of the relative vorticity at the surface. Relative vorticity is not a conserved quantity, but the same evolution was observed in the surface density distribution. In order to look at the details of the surface patterns generated from the instability, surface floats were distributed uniformly in the motionless part of the

surface ($y > 0$, $\rho = \rho_0$) at $t = 0$. A snapshot of the pattern generated by these passive tracers is shown in Figure 5. There is a strong horizontal convergence at the front $O(10^{-4}\mathrm{s}^{-1})$, accumulating floats that trace out the front, including spiral eddies at the scale of 10 km. At the time displayed, the concentration is about 75 times the initial at the main front and up to 50 at the spiral eddies. This convergence implies significant vertical downdrafts that are essential for the transformation from the (quasi-)linear regime displayed in Figure 3(b), to the fully developed cyclone in Figure 3(c) [3].

At later stages, $t \sim 18$ days, secondary instabilities set in and generate a more random eddy pattern [3]. This could account for the observations of less organized structures than displayed in Figure 1.

4. Conclusions

Spiral eddies are clearly observed in the experiment. From the given initial frontal configuration, their generation may be explained by a short scale, predominantly baroclinic, frontal instability. In the presence of surface floats, the front and the spiral eddies are associated with streaks that would make them detectable by remote sensing.

Acknowledgments. The authors thank Professor J. Berntsen for helping to set up the numerical experiment and Professor T. A. McClimans for valuable comments and suggestions in the preparation of this manuscript. The first author would also like to express his thanks to Dr K. Iga and Dr D. Renouard for fruitful discussions. This work has received support from The Research Council of Norway (Programme for Supercomputing) through a grant of computing time.

References

[1] P. Scully-Power. Navy Oceanographer Shuttle Observations, STS 41-G, Mission Report. Technical Report NUSC TD 7611, Naval Underwater Systems Center, New London, Connecticut, 1986.

[2] S. T. Dokken and T. Wahl. Observations of spiral eddies along the Norwegian coast in ERS SAR images. Technical Report 96/01463, Norwegian Defence Research Establishment (NDRE), 1996.

[3] T. Eldevik and K. B. Dysthe. On spiral eddies in the ocean. In preparation, 1998.

[4] D. C. Honhart, editor. *Oceanography from the Space Shuttle.* University Corporation for Atmospheric Research and the Office of Naval Research, United States Navy, Boulder, Colorado, 1989. URL: http://-daac.gsfc.nasa.gov/CAMPAIGN_DOCS/OCDST/shuttle_oceanography_web/oss_cover.html.

[5] C. Y. Shen and T. Evans. Submesoscale dynamics and sea surface spiral eddies. Abstract for the IAPSO in Hawaii, Symposium PS-08, 1995.

[6] P. K. Kundu. *Fluid Mechanics.* Academic Press, San Diego, California, 1990.

[7] R. D. Pingree. Cyclonic eddies and cross-frontal mixing. *J. Mar. Biol. Ass. U.K.*, 58:955–963, 1978.

[8] J. Bjerknes. On the structure of moving cyclones. *Geof. publ.*, 1(2), 1919.

[9] J. Tintore, P. La Violette, I. Blade, and A. Cruzado. A study of an intense density front in the Eastern Alboran Sea: The Almeria-Oran front. *J. Phys. Oceanogr.*, 18:1384–1397, 1988.

[10] I. Orlanski. Instability of frontal waves. *J. Atmos. Sci.*, 25:178–200, 1968.

[11] K. Iga. Reconsideration of Orlanski's instability theory of frontal waves. *J. Fluid Mech.*, 255:213–236, 1993.

[12] N. Paldor and M. Ghil. Shortwave instabilities of coastal currents. *Geophys. Astrophys. Fluid Dyn.*, 58:225–241, 1991.

[13] P. D. Killworth, N. Paldor, and M. E. Stern. Wave propagation and growth on a surface front in a two-layer geostrophic current. *J. Mar. Res.*, 42:761–785, 1984.

[14] J. Berntsen, M. D. Skogen, and T. O. Espelid. Description of a σ-coordinate ocean model. Technical Report ISSN 0071-5638, Institute of Marine Research, Bergen, Norway, 1996.

[15] I. Orlanski and M. D. Cox. Baroclinic instability in ocean currents. *Geophys. Fluid Dyn.*, 4:297–332, 1973.